

On the Return Distributions of a Basket of Cryptocurrencies and Subsequent Implications

(First Draft: May 14, 2021)

Christoph J. Börner^a, Ingo Hoffmann^a, Jonas Krettek^a, Lars M. Kürzinger^{a,*},
Tim Schmitz^a

^a*Financial Services, Faculty of Business Administration and Economics,
Heinrich Heine University Düsseldorf, 40225 Düsseldorf, Germany*

Abstract

This paper evaluates and assesses the risk associated with capital allocation in cryptocurrencies (CCs). In this regard, we take a basket of 27 CCs and the CC index EWCI⁻ into account. After considering a series of statistical tests we find the stable distribution (SDI) to be the most appropriate to model the body of CCs returns. However, as we find the SDI to possess less favorable properties in the tail area for high quantiles, the generalized Pareto distribution is adapted for a more precise risk assessment. We use a combination of both distributions to calculate the Value at Risk and the Conditional Value at Risk, indicating two subgroups of CCs with differing risk characteristics.

Keywords: Body-/Tail-Models, Cryptocurrencies, Index Construction, Market Segmentation, Statistical Tests

JEL Classification: C12, C13, C43, E22.

ORCID IDs: 0000-0001-5722-3086 (Christoph J. Börner), 0000-0001-7575-5537 (Ingo Hoffmann), 0000-0002-0978-6252 (Jonas Krettek), 0000-0001-5774-1983 (Lars M. Kürzinger), 0000-0001-9002-5129 (Tim Schmitz).

Acknowledgement: We thank Coinmarketcap.com for generously providing the cryptocurrency time series data for our research.

*Corresponding author. Tel.: +49 211 81-11515; Fax.: +49 211 81-15316

Email addresses: Christoph.Boerner@hhu.de (Christoph J. Börner),
Ingo.Hoffmann@hhu.de (Ingo Hoffmann), Jonas.Krettek@hhu.de (Jonas Krettek),
Lars.Kuerzinger@hhu.de (Lars M. Kürzinger), Tim.Schmitz@hhu.de (Tim Schmitz)

1. Introduction

Following the financial crisis of 2007 and a period of extreme uncertainty and volatility, trust in the financial system and its institutions, like central banks and their monetary policies, have been shattered (Kaya Soyly et al., 2020; Bouri et al., 2017a).

Against this background, the market for cryptocurrencies (CCs) started to emerge in 2009 with the development of the Bitcoin by Nakamoto (2008). This innovative peer-to-peer electronic cash system is not accountable to any subordinate institution, but is managed and controlled by its own community using the blockchain technology. Furthermore, the anonymity and security of transactions represent another noteworthy feature Bitcoin promises its users (Kakinaka and Umeno, 2020), resulting in increasing trading volumes and prices (Corbet et al., 2019). This development raises questions for both investors and regulators alike regarding the CC market’s characteristics and risk profile, which need to be answered in order for CCs to become an investable asset class for a broad audience (Gkillas and Katsiampa, 2018; Majoros and Zempléni, 2018; Osterrieder et al., 2017) and to provide guidance for risk management in general (Kakinaka and Umeno, 2020). In this regard, this study examines the question which class of distribution functions models CC returns most accurately. We answer this question using a novel approach to separate a distribution’s body from its tail proposed by Hoffmann and Börner (2021). By doing so we are able to determine the risk and statistical properties associated with CCs and provide valuable implications for portfolio management and regulators alike.

Even though the technical properties of CCs are well understood, CCs’ behavior remains to be fully comprehended and analyzed. As of today, many economic studies have focused on Bitcoin and other prominent CCs such as Ethereum and Ripple since they dominate the CC market due to their high proportion of total market capitalization (Glas, 2019). In this regard, Baur et al. (2018) and Glas (2019) find Bitcoin and other CCs to be uncorrelated to traditional assets in times of financial distress. Additionally, Gkillas et al. (2018), show CC’s behavior to differ from fiat currencies as well. Furthermore, various studies analyze certain characteristics of CCs like e.g. volatility (Polasik et al., 2015; Balcilar et al., 2017), diversification issues (see i.a. Brière et al. (2015); Selgin (2015); Corbet et al. (2018)) and safe haven properties (Bouri et al., 2017b; Urquhart, 2018)¹.

However, in order to evaluate the corresponding market risk and to completely understand the CC market as a whole, we follow other studies in analyzing return distributions of the CC market. As numerous studies observe non gaussian behavior and heavy tails in return distributions (Osterrieder et al., 2017; Gkillas et al., 2018; Gkillas and Katsiampa, 2018), a distribution model accounting for these observed characteristics ought to be implemented. To account for these properties Majoros and Zempléni (2018) and Kakinaka and Umeno

¹For a more extensive literature review, see Corbet et al. (2019).

(2020) utilize the class of stable distributions (SDIs) in their recent studies. However, Kakinaka and Umeno (2020) observe the SDI to be unable to efficiently grasp the heavy tails of the analyzed return distributions in all scenarios in comparison to other possible distributions. Given this background, the generalized Pareto distribution (GPD), a statistical distribution which appears to model heavy tail properties more accurately, is used in further studies (Gkillas et al., 2018; Gkillas and Katsiampa, 2018). Following the approach presented in Hoffmann and Börner (2021), we therefore attempt to use a combination of both described distributions. Analytically discovering the beginning of the tail of the analyzed return distributions, enables us to split the given data into a body and a tail for each of which we implement a different distribution. For the first sample, containing the tail of potential losses, we implement the GPD, since literature and our conducted tests show its goodness of fit for estimating tail values. For the remaining body of our data we apply the SDI as its fit outperforms other possible distributions.

Our study aims to add to the existing literature by implementing a novel approach, which tries to reach a higher quality of modelling return distributions observed in the CC market. Furthermore, as of today most studies are merely concerned with analyzing characteristics of Bitcoin or the most prominent CCs like i.a. Ethereum, Ripple and Litecoin ((Baur et al., 2018; Bouri et al., 2017b; Osterrieder et al., 2017; Gkillas et al., 2018; Gkillas and Katsiampa, 2018; Majoros and Zempléni, 2018; Kakinaka and Umeno, 2020)). Therefore, most studies do not consider the entirety of the CC market, which, as Glas (2019) points out, might lead to potential bias. Hence, we join Glas (2019) and ElBahrawy et al. (2017), in an attempt to give a broader overview of the CC market. By doing so we tackle two existing gaps in literature found by Corbet et al. (2019) in their extensive literature review. Namely, we extend the number and size of analyzed data in an attempt to analyze CCs as an asset class. Furthermore, our research does provide practical relevance in form of an improved risk assessment. By analytically separating a distribution's body from its tail and implementing different distributions, we are able to estimate risk measures in form of the Value at Risk and the Conditional Value at Risk more precisely. Both of which do yield an importance for regulators and investors alike.

The remainder of this paper is structured as follows: In Sec. 2 we present and describe our data used for our following analysis. In Sec. 3 we perform a series of statistical analyses and tests which lead us to the family of SDIs as the best model choice for the body of the CCs returns distribution. Based on these findings, Sec. 4 is concerned with the assessment of the tail risk inherent in an investment in a single CC or the basket aggregated in the EWCI⁻. We compare both methods of the risk assessment at high quantiles. First we use the body model and second we adapt the GPD as tail model for risk assessment in terms of the Value at Risk and the Conditional Value at Risk. The last section summarizes our most important results and gives an overview of further research topics.

2. Data

As a foundation of our analysis, we follow various studies, by extracting CCs' daily prices from the website coinmarketcap.com (i.a. (Fry and Cheah, 2016; Hayes, 2017; Brauneis and Mestel, 2018; Caporale et al., 2018; Gandal et al., 2018; Glas, 2019)). For an observation period from 2014-01-01 to 2019-06-01, we take $N = 66$ CCs from the Coinmarketcap Market Cap Ranking at the reference date of 2014-01-01 into consideration, cf. Tab. 1.

In order to depict the CC market as a whole, we aim to include as many CCs in our analysis as possible. However, as data gaps appear in the time series of most CCs considered, we exclude all CCs with five or more consecutive missing observations. By utilizing the Last Observation Carried Forward (LOCF) approach, as previously done in Schmitz and Hoffmann (2020) and Trimborn et al. (2020), we are able to include all CCs with smaller data gaps.

After taking these considerations into account, 27 CCs remain in our data set, all of which are depicted in bold letters in cf. Tab. 1. In a next step, we convert the CC prices denoted in USD to EUR prices, using the daily USD-EUR exchange rates retrieved from Thomson Reuters Eikon. For the purpose of preventing potential weekday biases, the resulting (daily) observations are converted to weekly observations in a following step. In a final step, we calculate logarithmic returns using these weekly CC EUR prices for each CC, which we will refer to as returns in the remainder of this paper.

CC	ID	CC	ID	CC	ID
Anoncoin	ANC	Argentum	ARG	AsicCoin	ASC
BBQCoin	BQC	BetaCoin	BET	BitBar	BTB
Bitcoin	BTC	BitShares PTS	PTS	Bullion	CBX
ByteCoin	BTE	CasinoCoin	CSC	CatCoin	CAT
Copperlark	CLR	CraftCoin	CRC	Datacoin	DTC
Deutsche e-Mark	DEM	Devcoin	DVC	Diamond	DMD
Digitalcoin	DGC	Dogecoin	DOGE	Earthcoin	EAC
Elacoin	ELC	EZCoin	EZC	FastCoin	FST
Feathercoin	FTC	Fedoracoin	TIPS	FLO	FLO
Franko	FRK	Freicoi	FRC	Globalcoin	GLC
GoldCoin	GLC	GrandCoin	GDC	HoboNickels	HBN
I0Coin	I0C	Infinitecoin	IFC	Ixcoin	IXC
Joulecoin	XJO	Junkcoin	JKC	Litecoin	LTC
LottoCoin	LOT	Luckycoin	LKY	Megacoin	MEC
MemoryCoin	MMC	MinCoin	MNC	Namecoin	NMC
NetCoin	NET	Noirbits	NRB	Novacoin	NVC
Nxt	NXT	Omni	OMNI	Orbitcoin	ORB
Peercoin	PPC	Philosopher Stones	PHS	Phoenixcoin	PXC
Primecoin	XPM	Quark	QRK	Ripple	XRP
SexCoin	SXC	Spots	SPT	StableCoin	SBC
TagCoin	TAG	Terracoin	TRC	Tickets	TIX
TigerCoin	TGC	WorldCoin	WDC	Zetacoin	ZET

Table 1: Considered CCs and depicted data set (bold type), data source: CoinMarketCap.

For an aggregated perspective on CCs, we use the above-mentioned weekly

CC data to calculate an Equally-Weighted CC Index (EWCI), as it is similarly done in Schmitz and Hoffmann (2020). Whereas, as we exclude more CCs in comparison to Schmitz and Hoffmann (2020), we will call this index $EWCI^-$ for a more precise distinction.

3. The return distribution of cryptocurrencies

For an initial classification of CCs simple statistical key figures from the standard repertoire of empirical statistics are used below. The description and evaluation of additional statistical properties of CCs, for example Value at Risk or lower-partial moments, are carried out using a suitable distribution function. Our results show that the family of SDIs is a suitable model for the examined returns of CCs. Hence, this family of distributions is used in Sec. 4 for a more in-depth analysis of the statistical properties of CCs.

3.1. Determination of basic statistical key figures of the cryptocurrencies

Standard procedures lead us to estimates of the set of basic statistical key figures: mean $\hat{\mu}$, variance $\hat{\sigma}^2$ and the bandwidth (Tab. 2.).

Crypto ID	Mean $\hat{\mu}$	Variance $\hat{\sigma}^2$	Bandwidth		HDS-Test		SIG-Test	
			min	max	H0	p-Value	H0	p-Value
EWCI ⁻	0.3	1.6	-40.8	37.7	0	79.2	0	10.8
ANC	-1.0	14.3	-241.4	162.9	0	99.0	0	17.1
BTB	-0.7	11.7	-201.2	150.4	0	97.4	0	37.2
BTC	0.9	1.0	-30.4	42.2	0	99.8	0	59.2
CSC	-1.2	30.5	-697.9	169.0	0	92.2	0	51.2
DEM	-1.4	9.3	-100.8	145.8	0	99.6	0	85.8
DMD	0.0	4.1	-84.7	102.1	0	99.0	0	43.9
DGC	-1.7	9.0	-217.4	116.2	0	96.6	0	31.1
DOGE	0.9	3.7	-60.8	144.9	0	97.6	1	0.1
FTC	-0.9	7.6	-144.7	171.7	0	83.2	0	10.8
FLO	0.7	6.8	-67.9	162.2	0	84.8	0	43.9
FRC	-0.5	21.3	-332.1	338.9	0	100.0	0	95.3
GLC	0.2	5.6	-74.1	91.0	0	100.0	0	51.2
IFC	-0.6	10.6	-126.4	296.1	0	50.0	0	51.2
LTC	0.6	2.1	-34.2	87.5	0	99.0	0	21.1
MEC	-1.6	5.6	-112.9	133.1	0	96.6	0	85.8
NMC	-0.9	3.0	-110.2	82.4	0	100.0	0	25.8
NVC	-1.0	5.5	-235.7	128.2	0	99.6	0	8.4
NXT	-0.1	4.2	-83.9	106.5	0	93.8	0	8.4
OMNI	-1.4	5.4	-73.1	116.9	0	82.6	0	43.9
PPC	-0.9	2.7	-60.2	73.8	0	86.8	0	21.1
XPM	-1.0	4.1	-67.7	117.7	0	91.2	1	4.9
ORK	-1.1	7.2	-94.1	137.9	0	96.8	0	37.2
XRP	1.1	3.8	-72.9	109.7	0	100.0	1	0.0
TAG	-1.1	5.3	-63.6	136.3	0	100.0	0	59.2
TRC	-1.0	6.7	-72.7	162.6	0	94.6	0	17.1
WDC	-1.6	6.8	-121.7	110.3	0	99.8	0	51.2
ZET	-1.0	6.6	-97.7	131.4	0	94.8	0	95.3

Table 2: Basic statistical key figures and tests on unimodality and symmetry. Units in percent and boolean, see text.

It can be seen that the returns scatter strongly around a centre close to zero. While the variance and thus the standard deviation indicate leptokurtic behavior and therefore a concentration of returns, the sometimes considerable bandwidth indicates a strong blur of returns over a wide measurement range. This leads to the preliminary conclusion that the returns of CCs in the middle value range follow a concentrated distribution that has pronounced fat tails in the outer areas. In particular, the large variance ($\sim 7\%$) and the bandwidth ($\sim 300\%$) of CCs clearly show the completely different character of CCs compared to traditional asset classes. Comparable values on a weekly basis for the traditional asset classes (stocks, bonds, real estate, etc.) fall in the range of $\sim 0.02\%$ (variance) or $\sim 0.1\%$ (bandwidth) on average. Hence, in comparison it can be seen that there is a considerable risk associated with CCs.

Additionally, in this step we use the Hartigan dip test (Hartigan and Hartigan, 1985) to test the null hypothesis H0 that the empirical distribution is unimodal and symmetric. So for each data set the Hartigans Dip Statistics (HDS) are calculated and evaluated. To test for symmetry, the simple sign test, cf. e.g.

Gibbons and Chakraborti (2011), is carried out for each data set. The last four columns in Tab. 2 show the results of the both tests.²

The results and especially the high p -values of the HDS-Test strongly suggest all data sets to obey a unimodal distribution. The CC Infinitecoin (IFC) shows the lowest p -value. This indicates that the empirical distribution could be multimodal. In fact, the histogram of returns for the IFC suggests a multi-peak nature. There are no indications of a fundamental structural break, so this tends to be more of a random nature and is due to insufficient statistics (cf. theorem of Glivenko (1933); Cantelli (1933)), which might occur with short samples in particular. When adjusting a unimodal distribution function later in Sec. 3.3, we expect a lower quality of the distribution model for the returns of this currency.

Apart from three exceptions, a clear result can also be seen in the SIG-Test for symmetry of the empirical distribution of returns. For the vast majority of CCs, the assumption of a symmetrical distribution of returns at a moderately high level of significance cannot be rejected. While the assumption of a symmetrical distribution of the returns is narrowly rejected for the CC Primecoin (XPM), the rejection for the CCs Dogecoin (DOGE) and Ripple (XRP) is almost clear. We therefore assume that the distributions are slightly skewed.

Going forward, we assume the returns of the CCs to be concentrated around zero and the empirical distribution to have a fat tail due to the large bandwidth. Furthermore, we expect the empirical distribution to have a unimodal and essentially symmetrical shape. Anyway, it cannot be ruled out that the data sets in question may be (slightly) skewed. We will take this fact into account when selecting and adapting a suitable distribution function in Section 3.3.

3.2. Statistical tests to further reduce the variety of possible distributions

A large number of mathematical models are available for the statistical description of CC returns. On the basis of some characteristic features of the data set, the family of models can be narrowed down and a suitable family of functions for representing the distribution can be deduced. In the following a series of statistical tests are carried out in order to infer possible function families for the description of our data sets. The same tests are also carried out for the EWCI⁻ defined in Sec. 2. In total, $N = 28$ time series are considered in the tests described below.

Overall, the statistical tests in Sec. 3.1 and the following are used to examine whether the combined hypothesis that the data sets have a unimodal, symmetrical and stationary distribution must be rejected. Furthermore, it is checked whether the hypothesis of an independent, identical distribution (IID) of the individual returns must be rejected, which is an important property required to specify a distribution function.

²Note that for all tests performed in this paper, the following applies: The boolean "0" indicates that the null hypotheses cannot be rejected on a 5%-level and alternatively the boolean "1" indicates a rejection.

The augmented Dickey-Fuller test (Dickey and Fuller, 1979; Wooldridge, 2020) is used to test a possible rejection of the stationarity hypothesis. Finally, the ARCH test according to Engle (Engle, 1982, 2002) is used to check whether the hypothesis of homoscedasticity of the innovation process ϵ_t for the individual CCs and the EWCI⁻ must be rejected.

Augmented Dickey-Fuller Test

The augmented Dickey-Fuller test (ADF) is performed considering the autoregressive model for the CC return time series, y_t , of each CC³:

$$y_t = c + \delta t + \varphi y_{t-1} + \beta_1 \Delta y_{t-1} + \beta_2 \Delta y_{t-2} + \dots + \beta_p \Delta y_{t-p} + \epsilon_t. \quad (1)$$

With drift coefficient c , deterministic trend coefficient δ , AR(1) coefficient φ and coefficients β_i for the lag terms $i = 1, \dots, p$ up to the order $p = 10$. In Eq. (1) ϵ_t denotes the innovation process. The aim of the test is to check the hypothesis of trend stationarity, i.e. $\delta = 0$ is the null hypothesis, in the tables denoted by H0, see e.g. Wooldridge (2020).

The Heatmap in Fig. 1 visualizes the structure of the fitted autoregressive

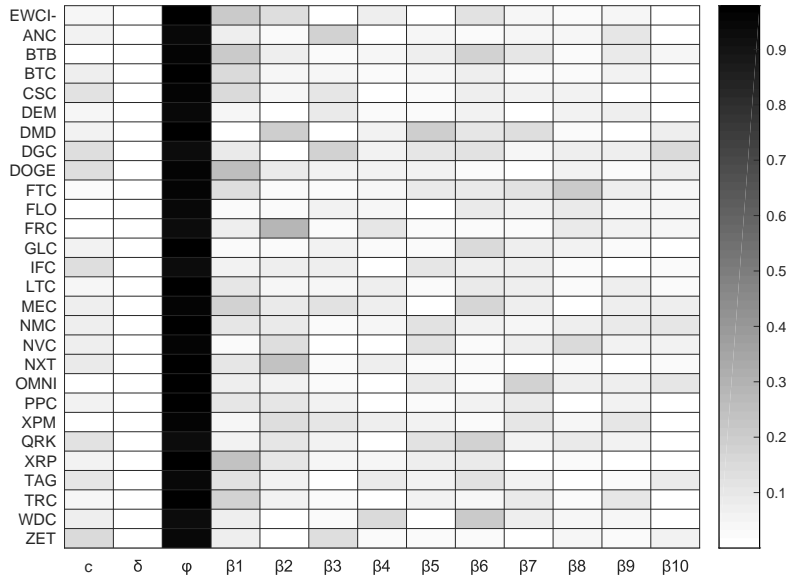


Fig. 1 The Heatmap reflects the structure of the autoregressive model with drift coefficient c , deterministic trend coefficient δ , AR(1) coefficient φ and coefficients β_i for the lag terms up to ten time shifts for each CC.

We find the deterministic trend coefficient δ to be comparable to zero in all CCs considered. The results in Tab. 3 in the first four columns provide a deeper

³Note, the returns r_t are calculated in this notation according to $r_t = y_t - y_{t-1}$.

insight. For the vast majority of CCs, the p -values are comfortably high, so that a rejection of the null hypothesis of trend stationarity is not indicated here. But as can be seen in the table the ADF-Test rejects the null hypothesis for the CCs FLO (FLO), Quark (QRK) and Worldcoin (WDC) on a 5% confidence level. At this point we take a closer look at the corresponding trend coefficients: $\delta_{\text{FLO}} = 1.6\text{e-}03$, $\delta_{\text{QRK}} = 1.5\text{e-}04$ and $\delta_{\text{WDC}} = 1.0\text{e-}04$. Since all the coefficients δ are close to zero, the influence of a possible trend is likely to be of significantly less importance. Therefore, in the following, we assume trend stationarity ($\delta = 0$) for the time series of CCs.

The third column in the Heatmap in Fig. 1 illustrates the value of φ . We find the parameter φ to be greater than 0.9 for all CCs and, for the most part, clearly close to 1. The latter is an important condition to be fulfilled for the assumption of a random walk ($\varphi = 1$).

The augmented Dickey-Fuller test was performed for lags p up to order ten. More complicated dynamics with serial correlation make themselves noticeable in the analysis by the fact that the coefficients of the terms corresponding to the lags are clearly different from zero. We find the absolute values of the coefficients (that means $|\beta_i|$) to be close to zero. In fact, the majority of the absolute coefficients $|\beta_i|$ are clearly smaller than 0.2 as an upper limit⁴ and a basic model $y_t = c + y_{t-1} + \epsilon_t$ can be assumed (in Tab. 3 third column denoted with "G"). Only a few single coefficients exceed the value 0.2 by a small margin and in these cases a model with a slightly influencing lag structure $y_t = c + y_{t-1} + \bar{\beta} \times (\text{Lag-Structure}) + \epsilon_t$ with an average coefficient $\bar{\beta} = 0.03$ could be guessed at. By marking the corresponding CCs with "L", Tab. 3 shows for which CCs this is the case.

Due to the observed insignificance of the lag structure, we assume a basic model "G" in these cases as well and expect statistical inaccuracies to distort the result due to the limited length of the time series. We therefore postulate a possible serial correlation in the data sets to be of minor importance. Thus, the detailed analysis of the results of the augmented Dickey-Fuller test suggests that the model $r_t = c + \epsilon_t$ cannot not be rejected for the returns r_t . Here, c denotes the individual time-constant drift term for each CC and, as above, ϵ_t denotes the innovation process.

Test on autoregressive conditional heteroscedasticity

The ARCH-Test is performed for time shifts q up to the order of ten. Up to this lag, the null hypothesis that the innovation process of returns is homoscedastic could not be rejected for most CCs (see Tab. 3), i.e. the basic model $\epsilon_t = \sigma z_t$ with constant volatility σ and z_t being an independent and identical distributed process with mean 0 and variance 1 could not be rejected for the majority of CCs. Note, that the results found in literature show a het-

⁴By similar argumentation as in Wooldridge (2020, Chapter 11 therein) a repeated substitution causes the effectiveness of the corresponding terms to fall below the 5% mark in the next time step and thus become largely insignificant.

erogeneous picture and we do not find ARCG effects in contrast to other related studies (Peng et al., 2018; Dyrberg, 2016; Avital et al., 2014). After all, only 13 of 28 time series examined show ARCH effects and only in 8 cases clearly. The differences in studies may derive from different sampling frequencies or the differently chosen time period or its length and show that the design of the data collection may have an influence on the results.

CC ID	ADF-Test			ARCH-Test		Distribution
	H0	Model	<i>p</i> -Value	H0	<i>p</i> -Value	
EWCI ⁻	0	L	29.4	1	0.0	-
ANC	0	G	11.7	0	6.6	IID
BTB	0	L	22.9	1	0.0	-
BTC	0	G	48.7	1	3.1	≈ IID
CSC	0	G	49.2	0	50.8	IID
DEM	0	G	24.0	1	0.0	-
DMD	0	G	75.8	0	18.0	IID
DGC	0	G	11.0	1	0.0	-
DOGE	0	L	14.7	0	69.8	IID
FTC	0	L	14.9	1	0.0	-
FLO	1	L	4.0	0	63.2	≈ IID
FRC	0	L	14.3	0	71.6	IID
GLC	0	G	65.2	0	16.6	IID
IFC	0	G	6.4	0	38.3	IID
LTC	0	G	34.2	0	25.2	IID
MEC	0	G	17.7	1	1.5	≈ IID
NMC	0	G	42.0	0	38.1	IID
NVC	0	G	22.8	0	92.6	IID
NXT	0	L	50.4	1	0.0	-
OMNI	0	G	35.7	0	70.2	IID
PPC	0	G	41.5	1	0.4	≈ IID
XPM	0	G	12.7	0	11.1	IID
QRK	1	L	2.0	1	0.3	≈ IID
XRP	0	L	35.1	1	0.0	-
TAG	0	G	6.0	0	60.4	IID
TRC	0	G	46.0	1	1.9	≈ IID
WDC	1	L	2.5	1	0.0	-
ZET	0	G	22.6	0	6.0	IID

Table 3: Results of the statistical tests. Units in percent and boolean, see text.

The aforementioned results would justify the following calculation: $E[r_t] = \mu = c$ and $\text{Var}[r_t] = \sigma^2$ for the corresponding CCs. Estimates for the mean and the variance of the individual returns are noted in Tab. 2. Their calculation is also justified with the combined consideration of the test results described above.

Combining both tests, we have noted a characterization of the return distribution in the last column of Tab. 3. For the majority of CCs, independent and identical distributed (IID) returns can be assumed. Another part is approximately independent and identical distributed (≈ IID), because either the lag structure is less important in the ADF model or the rejection of homoscedastic-

ity based on the p -value is only weakly justified. For eight CCs the assumption of IID returns is clearly rejected.

Note, that the test for independently distributed returns could have been carried out with a turning point test (Bienaymé, 1874; Kendall and Stuart, 1977). However, as we are interested in a deeper analysis of the possible serial correlation in our data sets, we use a combination of the augmented Dickey-Fuller test and the ARCH-Test instead.

All tests carried out so far, do not reject the assumption that the returns obey an essentially symmetrical, unimodal distribution. Furthermore, for the majority of CCs the assumption of IID or nearly IID holds. In the first case (IID), the modeling of the empirical distribution with a distribution function is justified. In the second case (\approx IID), the model represents a coarser approximation. In the latter case, if the assumption of IID was to be rejected, the distribution function can only be used as a rough approximation and must be – just like the case (\approx IID) – examined more precisely and critically in individual cases as we show in the following section.

3.3. Determination of the appropriate return distribution function

When modeling the empirical distribution of returns, we focus on families of unimodal distribution functions that are defined over the entire axis (infinite support). Hence, a more detailed investigation of the following distribution functions suggests itself: normal distribution (N), the generalized extreme value distribution (GED), the generalized logistic distribution type 0 and type 3 (GLD0, GLD3) and the SDI. The analysis below proves that the family of SDIs is the most promising for modeling the distribution of CC returns. Therefore, this family of functions will be introduced here in more detail. Several different parametrizations exist for the SDI. In the following formulation we follow the presentation and the SDI's parametrization described in Nolan (2020, Def. 1.4 therein).

SDIs represent a class of distributions suitable for modeling heavy tails and skewness. A linear combination of two independent, identically and stable distributed random variables has the same distribution as the individual variables. A random variable X follows the SDI $S(\alpha, \beta, \gamma, \delta)$ if its characteristic function is given by:

$$\begin{aligned} E[\exp(itX)] = & \\ & \begin{cases} \exp\left(i\delta t - |\gamma t|^\alpha \left[1 + i\beta \text{sign}(t) \tan\left(\frac{\pi\alpha}{2}\right) \left(|\gamma t|^{1-\alpha} - 1\right)\right]\right) & \alpha \neq 1 \\ \exp\left(i\delta t - |\gamma t| \left[1 + i\beta \text{sign}(t) \frac{2}{\pi} \ln(|\gamma t|)\right]\right) & \alpha = 1 \end{cases} \end{aligned} \quad (2)$$

The first parameter $0 < \alpha \leq 2$ is called shape parameter and describes the tail of the distribution. This parameter may also be denoted as an *index of stability* or as a *characteristic exponent*. The second parameter $-1 \leq \beta \leq +1$ is a skewness parameter. If $\beta = 0$, then the distribution is symmetric otherwise it is left-skewed ($\beta < 0$) or right-skewed ($\beta > 0$). When α is small, the skewness

of β is significant. As α increases, the effect of β decreases. Further, $\gamma \in \mathbb{R}^+$ is called the scale parameter and $\delta \in \mathbb{R}$ is the location parameter.

For the special case $\alpha = 2$ the characteristic function Eq. (2) reduces to $E[\exp(itX)] = \exp(i\delta t - (\gamma t)^2)$ and becomes independent of the skewness parameter β and the SDI becomes equal to N with mean δ and standard deviation $\sigma = \sqrt{2}\gamma$.

Evaluation of distance measurements to compare model quality

In the following we use standard distance measures to determine and compare the model qualities of N, GED, GLD0, GLD3 and SDI for the individual CCs. There are several distance measures available which are suitable to measure the "discrepancy" between the empirical distribution function and a modelled distribution function. The distance measures from Cramér (1928) von Mises (1931) (W^2 -Distance), Anderson and Darling (1952, 1954) (A^2 -Distance) and Kolmogorov (1933) Smirnov (1936, 1948) (KS-Distance) are widely used in literature. A brief summary of the used distance measures are given in Appendix A.

In Tab. 4 we summarize the results for the Anderson Darling distance (A^2). The results for the Kolmogorov Smirnov distance (KS) and the Cramér von Mises distance (W^2) are compiled in Tab. A.11 and Tab. A.10 in Appendix A.

The values of the various distance measures show that the GED is least suitable to model the empirical distribution function. This may derive from the fact that the GED contains a fundamental skewness, which can only be influenced slightly via a parameter selection. Further, as soon as the shape parameter becomes different from zero a fundamental change of the distribution model occurs and the definition interval on the x -axis becomes restricted. Additionally, associated with a change of sign of the shape parameter there is a fundamental change of the distribution model as well and an abrupt change of the sign of the upper (or lower) bound on the x -axis, see e.g. Embrechts et al. (1997). In the present case, these properties of the GED make it difficult to precisely adapt the distribution to the data set.

On closer inspection of the calculated distances, the N does not appear to be suitable as a model either, since it is neither suitable for the modeling of empirical distribution functions with fat tails nor for those with a slight skew. Overall, the GLD0 shows significantly smaller distances across all CCs, but is also not ideally suited, as it is completely symmetrical and is therefore not able to model any slight skewness. The best results in terms of the smallest distance can be achieved with the GLD3 and with the SDI. When comparing all CCs, the corresponding distances are very close to each other. If only the Cramér von Mises distance and the Kolmogorov Smirnov distance are considered, see Appendix A, it turns out that around half of the empirical distributions of CC returns can be modeled with one or the other distribution. But as soon as more attention is paid to the tail, i.e. if deviations in the tail area are to be weighted more heavily in order to account for tail risks, and the Anderson Darling distance A^2 is considered, the share of CCs, for which the SDI is the most suitable model, predominates.

CC ID	Anderson Darling Distance A^2					Best Choice
	N	GED	GLD0	GLD3	SDI	
EWCI ⁻	3.41	147.4	1.76	0.81	0.79	SDI
ANC	8.65	22.4	2.53	1.61	0.39	SDI
BTB	3.36	12.3	0.76	0.48	0.22	SDI
BTC	2.07	224.8	0.88	0.60	0.97	GLD3
CSC	21.80	42.6	3.90	n.d.	0.43	SDI
DEM	2.64	6.7	0.54	0.17	0.20	GLD3
DMD	3.80	23.7	1.25	0.29	0.54	GLD3
DGC	6.84	26.6	2.05	0.65	0.78	GLD3
DOGE	9.56	9.1	4.10	1.77	0.53	SDI
FTC	9.41	14.2	1.77	1.05	0.17	SDI
FLO	1.74	1.5	0.54	0.54	0.32	SDI
FRC	17.36	n.d.	5.21	1.98	0.39	SDI
GLC	1.53	16.8	0.40	0.19	0.42	GLD3
IFC	n.d.	n.d.	4.79	3.43	2.57	SDI
LTC	7.10	13.7	2.72	0.72	0.71	SDI
MEC	9.19	18.8	3.71	1.25	0.45	SDI
NMC	6.02	60.5	1.73	0.48	0.47	SDI
NVC	17.24	51.3	4.08	1.47	0.47	SDI
NXT	6.69	17.6	2.39	0.96	0.41	SDI
OMNI	1.25	4.4	0.25	0.24	0.24	SDI
PPC	4.93	31.9	1.63	0.61	0.48	SDI
XPM	5.66	5.0	1.53	0.67	0.27	SDI
QRK	6.32	9.5	2.12	0.53	0.52	SDI
XRP	13.90	13.0	5.71	2.79	0.62	SDI
TAG	4.85	5.4	1.23	0.30	0.64	GLD3
TRC	4.36	5.5	0.80	0.45	0.13	SDI
WDC	9.68	24.1	3.95	1.35	0.57	SDI
ZET	5.23	12.3	1.58	0.41	0.48	GLD3

Table 4: Anderson Darling Distance for different body model distributions.

This result ties in with the results of Majoros and Zempléni (2018); Kakinaka and Umeno (2020). Using intraday and daily time series for a small sample of CCs they show the SDI family to be the best choice for modeling the empirical distribution function of intraday and daily returns of CCs.

For a broader sample of CCs we found that the SDI is, on average, much better suited to model both slight skewness and pronounced tails in the empirical distribution function. Therefore we use the SDI for all CCs to model the distribution function of returns.

The stable distribution family as a model for cryptocurrencies

Tab. 5 shows the results of the parameter estimation for the SDI $S(\alpha, \beta, \delta, \gamma)$.

CC ID	Parameter of the SDI $S(\alpha, \beta, \delta, \gamma)$								AD-Test	
	$\hat{\alpha}$	$\pm\Delta\alpha$	$\hat{\beta}$	$\pm\Delta\beta$	$\hat{\gamma}$	$\pm\Delta\gamma$	$\hat{\delta}$	$\pm\Delta\delta$	H0	p -Value
EWCI	1.62	0.18	0.46	0.39	0.07	0.01	-0.01	0.02	0	48.9
ANC	1.41	0.17	0.26	0.31	0.16	0.02	-0.03	0.03	0	85.8
BTB	1.67	0.18	0.38	0.45	0.18	0.02	-0.03	0.04	0	98.3
BTC	1.78	0.16	-0.21	0.61	0.06	0.01	0.01	0.01	0	37.5
CSC	1.45	0.18	0.27	0.32	0.16	0.02	-0.04	0.03	0	81.4
DEM	1.65	0.18	-0.04	0.45	0.17	0.02	-0.01	0.03	0	99.0
DMD	1.56	0.18	0.10	0.39	0.11	0.01	-0.01	0.02	0	70.7
DGC	1.57	0.18	0.31	0.38	0.14	0.02	-0.04	0.03	0	49.7
DOGE	1.33	0.17	0.35	0.27	0.08	0.01	-0.02	0.02	0	72.0
FTC	1.63	0.18	0.54	0.38	0.12	0.01	-0.05	0.03	0	99.7
FLO	1.88	n.d.	1.00	n.d.	0.16	n.d.	-0.02	n.d.	0	92.3
FRC	1.24	0.16	0.06	0.26	0.13	0.02	-0.02	0.03	0	86.0
GLC	1.80	0.16	0.43	0.63	0.15	0.02	-0.02	0.03	0	82.5
IFC	1.47	0.18	0.25	0.33	0.12	0.01	-0.04	0.02	1	4.6
LTC	1.37	0.17	0.06	0.30	0.06	0.01	-0.01	0.01	0	55.2
MEC	1.25	0.16	-0.01	0.26	0.09	0.01	-0.02	0.02	0	79.9
NMC	1.48	0.18	0.07	0.34	0.08	0.01	-0.01	0.02	0	78.0
NVC	1.42	0.17	0.28	0.31	0.08	0.01	-0.03	0.02	0	77.5
NXT	1.48	0.18	0.37	0.32	0.10	0.01	-0.03	0.02	0	83.8
OMNI	1.82	0.16	0.26	0.71	0.14	0.01	-0.03	0.03	0	97.7
PPC	1.50	0.18	0.10	0.35	0.08	0.01	-0.02	0.02	0	76.8
XPM	1.58	0.18	0.42	0.37	0.10	0.01	-0.04	0.02	0	95.6
QRK	1.45	0.18	0.17	0.33	0.12	0.02	-0.03	0.02	0	72.6
XRP	1.33	0.17	0.35	0.27	0.07	0.01	-0.03	0.01	0	63.2
TAG	1.63	0.18	0.10	0.44	0.12	0.01	-0.02	0.02	0	61.1
TRC	1.64	0.18	0.29	0.43	0.13	0.02	-0.04	0.03	0	99.9
WDC	1.26	0.16	0.08	0.26	0.10	0.01	-0.03	0.02	0	67.2
ZET	1.53	0.18	0.15	0.36	0.13	0.02	-0.02	0.03	0	76.5

Table 5: Parameter of the SDI and goodness of fit test.

For the individual parameters of the SDI, the 95% scatter intervals are provided, as well. The latter can be determined from the covariance matrix of the estimated parameters. The covariance matrix of the parameter estimates is a matrix in which the off-diagonal element (i, j) resembles the covariance between the estimates of the i -th parameter and the j -th parameter. For the CC FLO, these scatter intervals cannot be determined numerically using the data set at hand. This is due to the fact that the corresponding empirical distribution on the far right shows a very long, pronounced tail and is strongly skewed to the right. The estimated parameter $\hat{\beta}$ of the SDI takes the value of 1 accordingly, see Tab. 5. It may be the case that the single right tail data point, i.e. the return in period 62, represents an outlier, which is difficult to determine and correct afterwards without any further knowledge.

On average, the estimated parameter $\hat{\alpha}$ exceeds 1.5. With parameter α increasing to its limit value of 2.0, it can be seen that the distribution function becomes similar to the N and the skewness parameter ($\beta \neq 0$) becomes increasingly insignificant. The parameters β and α of the SDI are mutually dependent and, as described above, the meaning of β decreases when α increases. So it is generally difficult to infer the skewness from the value β alone. A relative

comparison of the distributions with regard to the skewness is only possible if α has the same value. Hence, for a more precise analysis of a distribution's skewness, other methods are necessary. In this manner, we used the SIG-Test as an example and note the results in Tab. 2.

For some CCs and the EWCI⁻ index, Fig. 2 shows the empirical densities and the density of the corresponding SDI in comparison.

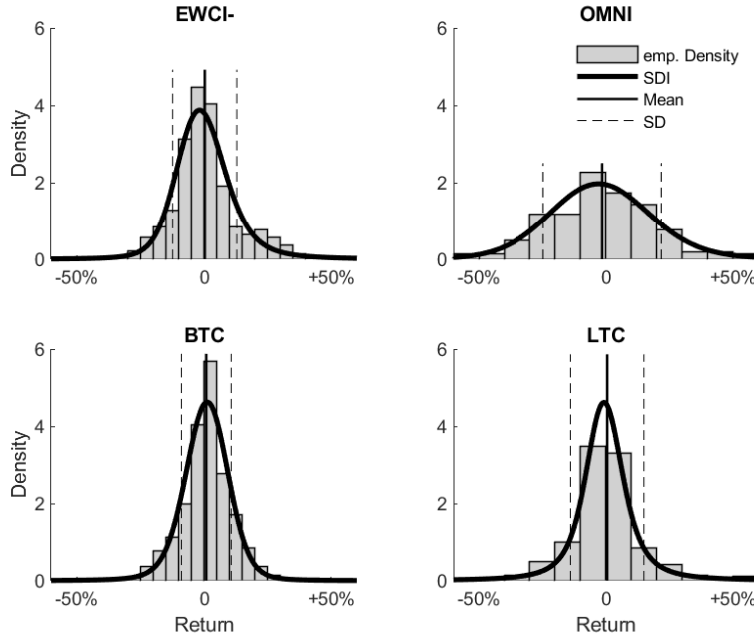


Fig. 2 The empirical densities as well as the results of the modeling of the distributions with the family of SDIs can be seen for the EWCI⁻ and selected CCs.

In addition, the complete goodness of fit test according to Anderson Darling was carried out. The last two columns of Tab. 5 show that for almost all CCs with very high significance (high p -values), the null hypothesis that the adjusted SDI models the data set cannot be rejected. Only for the CC Infnitecoin (IFC) this assumption is rejected at the 5% level. This is probably due to the fact that the empirical distribution suggests a slight bimodal distribution. This peculiarity of the CC Infnitecoin is also indicated in the results of the HDS-Test in Tab. 2.

Overall, it can be stated that the SDI family represents a suitable framework for modeling the distribution function of CC returns. We will make use of this finding for the assessment of tail risks and the comparison of our results with other modeling approaches.

4. Assessment of tail risks

4.1. Modeling of cryptocurrencies' tail risks

Especially when considering high quantiles in the risk assessment process, separate modeling of the tail of the often unknown parent distribution is necessary. In practice, the GPD is used predominantly as a tail model (Basel Committee on Banking Supervision, 2009). Henceforth, we briefly discuss the main steps of the tail modelling using the GPD in this section.

A theorem in extreme value theory, which goes back to Gnedenko (1943), Balkema and de Haan (1974) and Pickands III (1975), states that for a broad class of distributions, the distribution of the excesses over a threshold u converges to a GPD if the threshold is sufficiently large.

The GPD is usually expressed as a two-parameter distribution and follows the distribution function:

$$F(x) = 1 - \left(1 + \xi \frac{x}{\sigma}\right)^{-\frac{1}{\xi}}, \quad (3)$$

where σ is a positive scale parameter and ξ is a shape parameter (sometimes called the *tail parameter*). The density function is described as

$$f(x) = \frac{1}{\sigma} \left(1 + \xi \frac{x}{\sigma}\right)^{-\frac{1+\xi}{\xi}}, \quad (4)$$

with support $0 \leq x < \infty$ for $\xi \geq 0$ and $0 \leq x \leq -\frac{\sigma}{\xi}$ when $\xi < 0$. The mean and variance are depicted as $E[x] = \frac{\sigma}{1-\xi}$ and $\text{Var}[x] = \frac{\sigma^2}{(1-\xi)^2(1-2\xi)}$, respectively. Thus, the mean and variance of the GPD are positive and finite only for $\xi < 1$ and $\xi < 0.5$, respectively. For special values of ξ , the GPD leads to various other distributions. When $\xi = 0, -1$, the GPD translates to an exponential or a uniform distribution. For $\xi > 0$, the GPD has a long tail to the right and resembles a reparameterized version of the usual Pareto distribution. Several areas of applied statistics have used the latter range of ξ to model data sets that exhibit this form of a long tail.

Since the GPD was introduced by Pickands III (1975), numerous theoretical advancements and applications have followed (Davison (1984), Smith (1984), Smith (1985), van Montfort and Witter (1985), Hosking and Wallis (1987), Davison and Smith (1990), Choulakian and Stephens (2001)). Its applications include the use in analysis of extreme events in hydrology, as a failure-time distribution in reliability studies and in the modeling of large insurance claims. Numerous examples of applications can be found in Embrechts et al. (1997) and the studies listed therein. The GPD is also increasingly used in financial and banking sectors. Especially in the assessment of risks based on high quantiles, the GPD is one of the proposed distributions for modeling the tail of an unknown parent distribution (Basel Committee on Banking Supervision, 2009).

The preferred method in literature for estimating the parameters of the GPD is the standard maximum likelihood method (Davison (1984), Smith (1984), Smith (1985), Hosking and Wallis (1987)). Choulakian and Stephens (2001)

state that it is theoretically possible to have data sets for which no solution to the likelihood equations exists, however this appears to be an extremely rare case in practice. In fact, in our examination of the 27 CCs and the EWCI⁻, maximum likelihood estimates of the parameters could be deduced in every case. Nevertheless, a plausibility check of the results is highly recommended. As we show in Sec. 4.2, when assessing tail risks, it is advisable to evaluate the results, in order to avoid possible misinterpretations in single individual cases.

For the separate modeling of the tail, solely the parameters of the GPD need to be determined from the data pertaining to the tail region of the underlying empirical distribution function, i.e. the data which belong to the area below a threshold u in case of the loss tail.

Tab. 6 depicts the estimated parameters for the GPD for the different CCs. The second column gives the proportion of the whole dataset belonging to the loss tail. The proportion of the return data below the threshold \hat{u} is used to fit the parameters ξ, σ of the GPD. The threshold value lies within the bandwidth shown in Tab. 2 and when considering the loss tail closer to the lower interval limit of the bandwidth. Due to the standard goodness of fit tests according to Crámer von Mises (CvM) or Anderson Darling (AD), the null hypothesis that the GPD is a suitable model for the tail, can not be rejected on any significance level. In addition, the p -values for the lower tail statistics (LT) according to Ahmad et al. (1988) are given in Tab. 6. The corresponding statistics AL^2 is defined in Appendix B and used here to determine the threshold value u . As can be seen in column six of Tab. 6 the lower tail statistics show high confidence levels, as well.

CC ID	Prop.	GPD-Parameter			Goodness of Fit		
		\hat{u}	$\hat{\xi}$	$\hat{\sigma}$	p -Values		
					LT	CvM	AD
EWCI ⁻	45.7	-1.7	-0.09	0.09	88.0	84.9	92.6
ANC	4.3	-52.0	-0.08	0.61	98.5	98.1	93.9
BTB	4.3	-51.0	0.63	0.13	99.0	96.1	98.1
BTC	24.1	-3.9	-0.30	0.10	93.0	97.5	98.1
CSC	9.9	-35.5	0.82	0.11	96.7	99.7	94.3
DEM	51.4	-1.3	-0.05	0.22	54.2	58.2	60.8
DMD	4.3	-32.5	0.04	0.13	94.5	89.0	93.2
DGC	10.3	-31.7	0.61	0.08	99.8	99.6	99.5
DOGE	21.6	-9.2	0.13	0.09	99.1	99.4	98.9
FTC	3.5	-37.0	0.99	0.05	99.7	99.4	93.7
FLO	16.3	-20.3	-0.25	0.17	93.9	91.5	89.2
FRC	11.0	-28.8	0.28	0.31	98.8	98.3	99.6
GLC	51.8	0.2	-0.19	0.20	99.9	99.9	100.0
IFC	20.9	-18.2	0.55	0.07	55.0	70.4	52.8
LTC	44.3	-0.7	-0.18	0.11	57.5	67.7	54.1
MEC	56.4	0.0	0.16	0.12	99.8	99.2	93.3
NMC	46.1	-1.9	0.15	0.09	78.0	95.7	94.0
NVC	9.2	-19.3	0.72	0.05	77.2	93.6	86.0
NXT	2.8	-34.6	1.27	0.03	60.1	76.7	67.7
OMNI	15.2	-23.0	-0.11	0.14	95.9	96.2	97.1
PPC	8.5	21.3	0.00	0.09	96.7	97.1	98.8
XPM	4.6	29.5	-0.08	0.12	91.4	93.1	96.7
QRK	63.5	-1.6	0.05	0.16	47.7	60.8	61.1
XRP	2.8	-25.6	0.76	0.04	99.2	98.8	99.1
TAG	53.2	-0.5	-0.13	0.17	91.2	92.7	96.8
TRC	35.5	-9.9	-0.06	0.15	64.2	70.9	81.0
WDC	62.8	0.8	0.18	0.13	94.8	94.4	88.9
ZET	20.9	-17.8	0.27	0.11	59.8	83.6	82.5

Table 6: Parameter of the GPD and goodness of fit test for the loss tail. Units in percent.

4.2. Risk assessment at high quantiles

In this section, we use the SDI as the body model and the GPD as the tail model to determine the risk parameters Value at Risk (as a quantile) and the Conditional Value at Risk (as a weighted loss when the loss threshold is exceeded), see i.a. Embrechts et al. (1997); Hull (2018). The data set includes $T = 282$ return observations for each CC, so that a comparison of the results with the empirically determined values is possible for moderately large confidence levels ($\approx 99\%$). The corresponding values for the confidence level of 99.9%, which is important for regulatory purposes (Basel Committee on Banking Supervision, 2004; European Parliament, 2009, 2013a,b), can only be estimated for data records of this length using a previously fitted body or tail model. The calculation of the quantiles is also subject to a statistical spread and the estimation error increases the fatter the tail is and the higher the confidence level is selected, see e.g. Hoffmann and Börner (2020b).

Value at Risk

Tab. 7 illustrates the results of the risk assessment for the most common confidence levels found in literature and regulatory requirements. The Value at Risk for the observed CCs are shown for the various model.

CC ID	Value at Risk empirical				Tail-Modell (GPD)				Body-Modell (SDI)			
	95%	97%	99%	99.9%	95%	97%	99%	99.9%	95%	97%	99%	99.9%
EWCI-	26	29	38	41	19	23	30	43	18	22	33	116
ANC	101	133	212	241	42	73	136	252	46	60	119	582
BTB	75	91	154	201	49	56	82	251	47	55	82	276
BTC	21	24	28	30	16	19	24	31	15	18	28	91
CSC	117	166	424	698	46	58	110	595	47	61	116	535
DEM	72	84	100	101	51	61	82	122	48	60	100	367
DMD	44	52	72	85	30	37	52	85	30	38	69	280
DGC	65	82	153	217	39	46	71	229	40	49	81	314
DOGE	36	43	56	61	23	29	42	77	23	31	64	343
FTC	50	60	109	145	36	38	50	205	32	37	53	177
FLO	49	54	66	68	38	44	55	70	37	42	52	68
FRC	110	142	256	332	57	78	136	333	54	79	185	1159
GLC	49	55	68	74	38	44	56	74	36	42	56	140
IFC	61	77	114	126	34	43	75	251	35	45	82	365
LTC	27	31	34	34	20	24	31	41	21	30	62	321
MEC	59	71	99	113	37	46	70	137	38	56	128	787
NMC	42	50	92	110	27	34	51	97	25	33	63	284
NVC	47	63	141	236	23	28	46	188	24	31	59	278
NXT	42	48	78	84	33	34	42	210	27	33	59	258
OMNI	48	55	67	73	37	43	55	76	37	42	56	142
PPC	35	40	55	60	26	31	41	61	25	33	60	258
XPM	40	46	62	68	29	35	47	70	27	33	51	191
QRK	62	71	91	94	41	50	70	117	38	50	96	440
XRP	30	36	57	73	24	25	32	85	22	30	61	330
TAG	47	53	62	64	35	41	53	73	34	42	69	252
TRC	51	57	69	73	37	44	57	83	36	44	68	238
WDC	64	79	109	122	39	50	76	150	40	57	128	769
ZET	59	73	91	98	37	46	70	151	37	47	85	357

Table 7: Value at Risk of the CCs for different confidence levels and different calculation methods. Losses with a positive sign and units in percent.

Overall, it can be seen that in the overwhelming number of individual cases, the assessment of risk with the tail model (GPD) is closer to the empirical Value at Risk values. This applies to the lower confidence levels in particular, but even with high confidence level of 99.9%, better estimates are possible in individual cases compared to the body model. This becomes apparent from the statistical parameters of the deviation analysis shown in Tab. 8 as well. The mean value and standard deviation over the set of CCs are shown. For this purpose, the deviation between the modeled variable and the corresponding empirical Value at Risks was determined. It turns out that, on average, adjusting the GPD as tail model leads to better risk estimates.

		ΔVaR		Confidence levels			
				95%	97%	99%	99.9%
Mean	GPD	./.	Emp.	0.5	-0.2	-4.6	15.5
	SDI	./.	Emp.	-0.3	0.4	10.5	214.1
SD	GPD	./.	Emp.	2.4	2.1	7.3	43.1
	SDI	./.	Emp.	1.8	4.1	19.3	211.7

Table 8: Average deviation from the empirical Value at Risk and scattering.

When comparing CCs with each other, a heterogeneous picture emerges, see Tab. 7. If the empirical Value at Risk for the 99.9% confidence interval is taken as a measure, two subgroups can be defined for the cut-off value $\text{VaR}_{99.9\%} \approx 100\%$. One group possesses a significantly lower tail risk ($\text{VaR}_{99.9\%} < 100\%$) as the corresponding $\hat{\xi}$ values in Tab. 6 indicate. The other group ($\text{VaR}_{99.9\%} > 100\%$) partly embodies a significantly higher tail risk. Correspondingly, large $\hat{\xi}$ values can be determined for these CCs.

Fig. 3 shows the empirical distribution function for the EWCI⁻ and Bitcoin (BTC), the SDI as a body model and the GPD as a tail model in comparison. The graphics on the right portray an enlargement of the loss area. Particularly in this region, the GPD models the empirical distribution function very well. Considering the afore conducted analysis, it can be stated that the GPD is ideally suited to carry out risk assessment at high quantiles. Therefore, we exclusively consider the GPD to estimate the Conditional Value at Risk as a further risk indicator in the following.

Conditional Value at Risk

The following Tab. 9 shows the Conditional Value at Risk calculated with the tail model (see Tab. 6) for the individual CCs. The calculation of the Conditional Value at Risk can be conducted using the mean excess function of the GPD:

$$e(v) = \frac{\sigma + \xi v}{1 - \xi}, \quad (5)$$

with v greater than the lower bound of the definition interval of the GPD considering the loss tail and the parameters σ, ξ of the GPD. The mean excess function is bound to the restrictions: $\xi < 1$, and $\sigma + \xi v > 0$, see e.g. Embrechts et al. (1997, Theorem 3.4.13). In Tab. 9 we used Eq. (5) to estimate the Conditional Value at Risk for each CCs setting $v = \text{VaR}_{p\%}$.

Once more, the grouping of CCs described above can be seen. A group of CCs with a fat tail and therefore higher tail risk can be distinguished from a group with moderate risk, see Tab. 9.

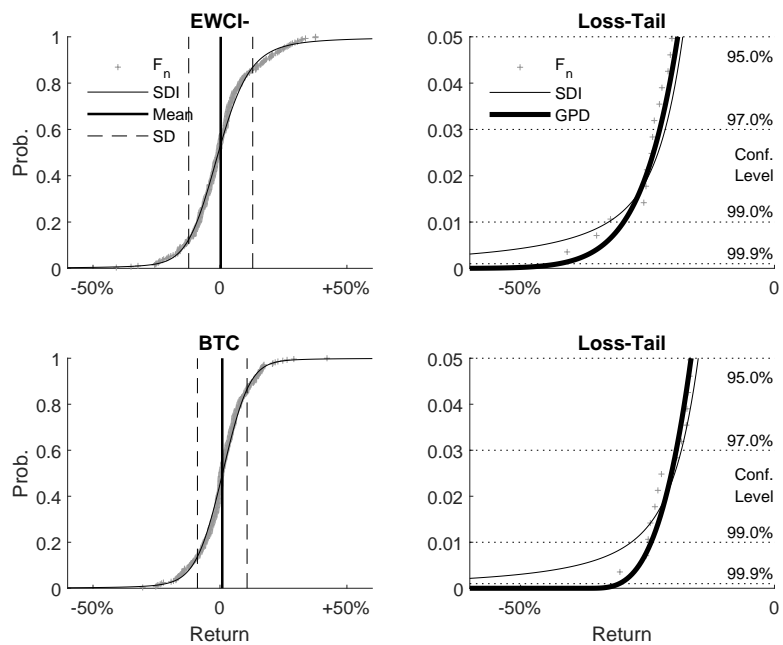


Fig. 3 The empirical distribution function and the distribution function modeled with the SDI can be seen for the EWCI⁻ and an exemplary selected CC (left panels). The right graphics focus on the loss tail. The GPD adapted as a tail model and the confidence levels that are important for the regulator are also shown.

CC ID	Conditional Value at Risk			
	95%	97%	99%	99.9%
EWCI-	25	29	35	47
ANC	96	125	184	292
BTB	169	188	258	717
BTC	20	23	26	31
CSC	308	374	655	3294
DEM	70	79	99	138
DMD	45	52	68	102
DGC	118	136	200	600
DOGE	37	43	59	98
FTC	3219	3408	4343	16648
FLO	44	49	58	69
FRC	122	151	231	504
GLC	49	54	64	79
IFC	91	112	181	571
LTC	26	29	35	44
MEC	59	70	99	178
NMC	43	51	71	125
NVC	99	115	180	679
NXT	-134	-138	-165	-784
OMNI	46	51	62	80
PPC	35	40	49	70
XPM	38	43	55	76
QRK	59	69	90	140
XRP	114	121	147	367
TAG	46	52	62	80
TRC	49	55	68	92
WDC	63	76	107	197
ZET	66	79	112	223

Table 9: Conditional Value at Risk of CCs for different confidence levels calculated with the corresponding tail model (GPD). Losses with a positive sign and units in percent.

Furthermore, two peculiarities are noticeable concerning the CCs Feathercoin (FTC) and Nxt (NXT). For both CCs, the tail is modeled on a small number of data points which have been assigned to the tail. This individual property of the data set deriving from the random distribution of the data in the tail area, is assumed to be given and, as already noted, is not corrected. In particular, when estimating the parameter ξ , small samples lead to large statistical errors. Regarding the conspicuous CCs, it can be observed that the parameter is very close to 1 in one case (FTC) and even higher in the other case (NXT), see Tab. 6. As a result, the calculation of the Conditional Value at Risk for the CC NXT is not possible and must be discarded, cf. Eq. (5) and the restriction $\xi < 1$. On the other hand, the calculation of the FTC with $\xi \approx 1$ has to be questioned critically. Hence, the Conditional Value at Risk may only be a rough estimate in this case.

5. Conclusion

This study aims to find a distribution which models CC returns most accurately and does not suffer from restrictions in specific parts of the distribution.

In former research the SDI and GPD have been found to model the body or the tail of the CC return distributions adequately respectively. Nevertheless both distributions prove to be unsuitable to model the entirety of the distribution appropriately. Therefore, using a novel approach to separate of distribution's tail from its body, we model the entire distribution by combining the model abilities of the SDI for the body and the GPD for the tail.

We select 27 CCs from the broad market of CCs according to predefined criteria and construct the representative index EWCI⁻. Overall, we find independent, identical distribution like the GPD and the SDI to be well suited for the most part and the family of SDIs in particular to be able to model the slightly skewed empirical distributions especially in the body region. A comparison between different distribution functions shows that the SDI has outstanding modeling properties across the entire data set. However, we show that the assessment of risks associated with fat tails can be carried out more precisely with the GPD. The analysis of tail risks in the CC market using the GPD further hints towards a certain internal structure of the CC market. It turns out that the CC market can roughly be divided into two sets: CCs with moderate risk and CCs with high risk. This finding provides valuable information for both investors and regulators alike. Hence, our results are not only relevant for scientific applications and extensions but for conceivable future regulation as well, if the asset class of CC is to become a permanent, noteworthy component of institutional investors' portfolios in the financial sector in the future. In this regard, numerous future extensions and topics of research are conceivable. On the one hand, the SDI's suitability to model CC returns in portfolio optimization remains to be investigated. On the other hand, further research considering the segmentation of the CC market could enrich the understanding of CCs and improve forecasts concerned with the fundamental behavior of different CCs.

Appendix A. Distance measures – Tables of results

Appendix A.1. Distance measures

In what follows a brief summary of the used distance measures is given.

Cramér von Mises and Anderson Darling distance measures

As a convenient measure of the distance or "discrepancy" between the empirical distribution functions $F_n(x)$ due to Kolmogorov (1933) and a model $F(x)$, usually the weighted mean square error is considered

$$\hat{R}_n = n \int_{-\infty}^{+\infty} (F_n(x) - F(x))^2 w(F(x)) dF(x), \quad (\text{A.1})$$

which was introduced in the context of statistical test procedures by Cramér (1928), von Mises (1931) and Smirnov (1936); compare also Shorack and Wellner (2009) and the references therein. In decision theory (Ferguson, 1967), the weighted mean square error has broad applicability in the determination of the unknown parameters of distributions via minimum distance methods (Wolfowitz,

1957; Blyth, 1970; Parr and Schucany, 1980; Boos, 1982). This measure of error is also used when adapting tail models (Hoffmann and Börner, 2020a, 2021). Therefore, in Sec. 4.1 we applied this error measure in connection with the adaptation of a suitable tail model for CC returns. A brief overview of the procedure to fit a suitable tail model is given in Appendix B.

The non-negative weight function $w(t)$ in Eq. (A.1) is a suitable preassigned function for accentuating the difference between the distribution functions in the range where the distance measure is desired to have sensitivity. Consider the weight function

$$w(t) = \frac{1}{t^a(1-t)^b} \tag{A.2}$$

for real-valued stress parameters $a, b \geq 0$ and $t \in [0, 1]$. Here, a affects the weight at the lower tail and b at the upper tail. Then, for $a = b = 0$, Eq. (A.1) provides the Cramér von Mises distance W^2 used in the corresponding statistic (Cramér, 1928; von Mises, 1931), whereas when heavily weighting the tails ($a = b = 1$), it is equal to the Anderson Darling distance A^2 used in the corresponding statistic (Anderson and Darling, 1952, 1954). The Anderson Darling distance weights the difference between the two distributions simultaneously more heavily at both ends of the distribution $F(x)$.

Cramér von Mises Distance

CC ID	Cramér von Mises Distance W^2					Best Choice
	N	GED	GLD0	GLD3	SDI	
EWCI ⁻	0.62	29.89	0.23	0.07	0.12	GLD3
ANC	1.51	4.25	0.41	0.24	0.06	SDI
BTB	0.55	2.22	0.11	0.06	0.04	SDI
BTC	0.40	41.81	0.16	0.11	0.19	GLD3
CSC	3.94	8.22	0.60	0.15	0.09	SDI
DEM	0.43	1.20	0.08	0.02	0.04	GLD3
DMD	0.70	5.19	0.22	0.05	0.10	GLD3
DGC	1.21	5.33	0.33	0.06	0.14	GLD3
DOGE	1.86	1.70	0.64	0.20	0.07	SDI
FTC	1.54	2.37	0.21	0.09	0.03	SDI
FLO	0.29	0.23	0.07	0.07	0.05	SDI
FRC	3.26	6.35	0.94	0.33	0.07	SDI
GLC	0.27	3.66	0.06	0.02	0.08	GLD3
IFC	2.92	4.43	0.91	0.72	0.58	SDI
LTC	1.35	2.98	0.46	0.11	0.12	GLD3
MEC	1.75	3.78	0.67	0.22	0.06	SDI
NMC	1.11	13.40	0.32	0.08	0.09	GLD3
NVC	3.09	10.46	0.65	0.17	0.09	SDI
NXT	1.20	3.57	0.33	0.09	0.07	SDI
OMNI	0.18	0.84	0.03	0.04	0.04	GLD0
PPC	0.88	7.07	0.26	0.09	0.08	SDI
XPM	0.99	0.86	0.20	0.05	0.05	SDI
QRK	1.15	1.74	0.36	0.08	0.10	GLD3
XRP	2.57	2.44	0.79	0.28	0.09	SDI
TAG	0.87	0.94	0.22	0.04	0.13	GLD3
TRC	0.71	0.96	0.09	0.04	0.02	SDI
WDC	1.80	5.03	0.70	0.23	0.10	SDI
ZET	0.92	2.33	0.25	0.05	0.09	GLD3

Table A.10: Cramér von Mises Distance for different body model distributions.

The results for the Anderson Darling distance are shown in Tab. 4 in the main text in Sec. 3.3.

Kolmogorov Smirnov distance measure

Furthermore, we also determine the well-known distance between the empirical distribution function and the distribution model due to Kolmogorov (1933) and Smirnov (1936, 1948). The Kolmogorov Smirnov distance (KS) calculates the supremum of the absolute difference between the empirical and the estimated distribution functions. Hence, the Kolmogorov Smirnov distance quantifies the "discrepancy" between the empirical distribution function of returns and the cumulative distribution function of the reference distribution, i.e. the model of the distribution function of CC returns s . A more theoretical overview and comparisons to other distance measures can be found in, e.g. Stephens (1974); Shorack and Wellner (2009).

Kolmogorov Smirnov Distance

CC ID	Kolmogorov Smirnov Distances KS					Best Choice
	N	GED	GLD0	GLD3	SDI	
EWCI ⁻	0.100	0.509	0.063	0.043	0.051	GLD3
ANC	0.132	0.233	0.069	0.070	0.047	SDI
BTB	0.087	0.156	0.056	0.037	0.042	GLD3
BTC	0.077	0.591	0.058	0.047	0.060	GLD3
CSC	0.179	0.296	0.085	0.053	0.047	SDI
DEM	0.071	0.127	0.048	0.027	0.039	GLD3
DMD	0.094	0.233	0.056	0.039	0.050	GLD3
DGC	0.117	0.241	0.066	0.034	0.045	GLD3
DOGE	0.159	0.132	0.099	0.053	0.042	SDI
FTC	0.134	0.141	0.061	0.045	0.031	SDI
FLO	0.069	0.060	0.036	0.035	0.038	GLD3
FRC	0.166	0.250	0.097	0.061	0.047	SDI
GLC	0.072	0.190	0.038	0.025	0.040	GLD3
IFC	0.194	0.251	0.142	0.144	0.106	SDI
LTC	0.133	0.184	0.077	0.043	0.058	GLD3
MEC	0.144	0.206	0.096	0.070	0.041	SDI
NMC	0.095	0.368	0.056	0.040	0.037	SDI
NVC	0.167	0.338	0.092	0.052	0.042	SDI
NXT	0.134	0.196	0.077	0.051	0.039	SDI
OMNI	0.052	0.113	0.028	0.031	0.036	GLD0
PPC	0.109	0.262	0.063	0.048	0.053	GLD3
XPM	0.116	0.095	0.055	0.048	0.035	SDI
QRK	0.108	0.139	0.073	0.048	0.048	SDI
XRP	0.171	0.168	0.101	0.061	0.039	SDI
TAG	0.101	0.103	0.056	0.037	0.048	GLD3
TRC	0.099	0.120	0.039	0.033	0.023	SDI
WDC	0.144	0.236	0.103	0.075	0.052	SDI
ZET	0.123	0.154	0.077	0.049	0.047	SDI

Table A.11: Kolmogorov Smirnov Distance for different body model distributions.

Appendix B. Modelling the tail of a distribution

For a very large class of parent distribution functions, the GPD can be used as a model for the tail, cf., e.g., Embrechts et al. (1997). This class of distributions includes all common parent distributions that play a role in the financial sector. Because of that, almost no uncertainty exists regarding the model selection for the tail of the unknown parent distribution. The required quantiles can then be determined to high confidence levels with sufficient certainty. A certain threshold thus divides the parent distribution into two areas: a body and a tail region. This approach is already common practice for calculating high quantiles more accurately, as indicated in European Parliament (2009).

Various authors have proposed methods for determining the appropriate threshold and subsequently the GPD as model for the tail from empirical data. Most methods require the setting of parameters, which often requires experience and hinders full automation of the modeling process. Based on ideas from Huisman et al. (2001); Longin and Solnik (2001); Chapelle et al. (2005);

Crama et al. (2007); Hoffmann and Börner (2018, 2020a) we use the following method for the determination of the tail model.

Given a suitable distance measure $\hat{R}_n = \hat{R}_n(F_n, \hat{F})$ as a function of the estimated GPD as a tail model $\hat{F}(x)$ and the empirical distribution function F_n due to Kolmogorov (1933), an automated modeling process can be constructed using the following algorithm.

1. Sort the random sample taken from an unknown parent distribution in descending order: $x_{(1)} \geq x_{(2)} \geq \dots \geq x_{(n)}$.
2. Let $k = 2, \dots, n$, and find, for each k , the estimates of the parameters of the GPD. Note: For numerical reasons, we start at $k = 2$.
3. Calculate the probabilities $\hat{F}(x_{(i)})$ for $i = 1, \dots, k$ with the estimated GPD, and determine the distance \hat{R}_k for $k = 2, \dots, n$.
4. Find the index k^* of the minimum of the distance \hat{R}_k .

Then, the optimal threshold value is estimated by $\hat{u} = x_{(k^*)}$, and the model of the tail of the unknown parent distribution is given by the estimated GPD $\hat{F}(x)$, which itself is determined from the subset $x_{(1)} \geq x_{(2)} \geq \dots \geq x_{(k^*)}$.

Chapelle et al. (2005) suggest using the mean squared error (MSE) as distance measure \hat{R}_n . Bader et al. (2018) implement a different algorithm based on sequences of goodness-of-fit tests. They use the Cramér-von Mises statistic and the Anderson-Darling statistic in combination with some beforehand set stopping rules. In contrast, we use the statistics AL_n^2 (lower tail) or its counterpart AU_n^2 (upper tail) due to Ahmad et al. (1988) as distance measure in the algorithm above.

The aforementioned distance measures are basing on the the weighted mean square error Eq. (A.1) The distance measures due to Ahmad et al. (1988) are derived from Eq. (A.1) when the integral is calculated with the weight functions Eq. (A.2) and $(a, b) = (1, 0)$ for the lower tail ($= AL^2$) and $(a, b) = (0, 1)$ for the upper tail ($= AU^2$).

This choice is justified as follows: The distance measure should take more account of the deviations between the measured data and the modeled data, especially in the tail area. This can be achieved with the asymmetrical weight functions – mentioned above – used in the weighted mean square error as distance measure \hat{R}_n , cf. e.g. Hoffmann and Börner (2018, 2020a). So, the distance measures AL_n^2 and AU_n^2 of Ahmad et al. (1988) take into account precisely the required asymmetrical weighting.

The pseudocode shown above was recently implemented in software packages and is available free of charge as a Python or R package, cf. [Zitate](#), [Links](#). The analysis shown in the main part was carried out with this packages.

References

- Ahmad, M.I., Sinclair, C.D., Spurr, B.D., 1988. Assessment of flood frequency models using empirical distribution function statistics. *Water Resources Research* 24, 1323–1328. doi:10.1029/WR024i008p01323.
- Anderson, T.W., Darling, D.A., 1952. Asymptotic theory of certain "goodness of fit" criteria based on stochastic processes. *The Annals of Mathematical Statistics* 23, 193–212. doi:10.1214/aoms/1177729437.
- Anderson, T.W., Darling, D.A., 1954. A test of goodness of fit. *Journal of the American Statistical Association* 49, 765–769. doi:10.2307/2281537.
- Avital, M., Leimeister, J.M., Schultze, U., 2014. ECIS 2014 proceedings: 22th European Conference on Information Systems ; Tel Aviv, Israel, June 9-11, 2014. AIS Electronic Library. URL: <http://aisel.aisnet.org/ecis2014/>.
- Bader, B., Yan, J., Zhang, X., 2018. Automated threshold selection for extreme value analysis via goodness-of-fit tests with application to batched return level mapping. *The Annals of Applied Statistics* 12, 310–329.
- Balcilar, M., Bouri, E., Gupta, R., Roubaud, D., 2017. Can volume predict bitcoin returns and volatility? a quantiles-based approach. *Economic Modelling* 64, 74–81. doi:10.1016/J.ECONMOD.2017.03.019.
- Balkema, A.A., de Haan, L., 1974. Residual life time at great age. *The Annals of Probability* 2, 792–804. doi:10.1214/aop/1176996548.
- Basel Committee on Banking Supervision, 2004. International convergence of capital measurement and capital standards - a revised framework.
- Basel Committee on Banking Supervision, 2009. Observed range of practice in key elements of advanced measurement approaches (ama).
- Baur, D.G., Dimpfl, T., Kuck, K., 2018. Bitcoin, gold and the us dollar—a replication and extension. *Finance Research Letters* 25, 103–110.
- Bienaymé, I.J., 1874. Sur une question de probabilités. *Bulletin de la Société Mathématique de France* 2, 153–154.
- Blyth, C.R., 1970. On the inference and decision models of statistics. *The Annals of Mathematical Statistics* 41, 1034–1058.
- Boos, D.D., 1982. Minimum anderson-darling estimation. *Communication in Statistics-Theory and Methods* 11, 2747–2774.
- Bouri, E., Gupta, R., Tiwari, A.K., Roubaud, D., 2017a. Does bitcoin hedge global uncertainty? evidence from wavelet-based quantile-in-quantile regressions. *Finance Research Letters* 23, 87–95. doi:10.1016/j.fr1.2017.02.009.

- Bouri, E., Molnár, P., Azzi, G., Roubaud, D., Hagfors, L.I., 2017b. On the hedge and safe haven properties of bitcoin: Is it really more than a diversifier? *Finance Research Letters* 20, 192–198. doi:10.1016/j.fr1.2016.09.025.
- Brauneis, A., Mestel, R., 2018. Price discovery of cryptocurrencies: Bitcoin and beyond. *Economics Letters* 165, 58–61.
- Brière, M., Oosterlinck, K., Szafarz, A., 2015. Virtual currency, tangible return: Portfolio diversification with bitcoin. *Journal of Asset Management* 16, 365–373.
- Cantelli, F.P., 1933. Sulla determinazione empirica delle leggi di probabilità. *Giornale dell’Istituto Italiano degli Attuari* 1933, 421–424.
- Caporale, G.M., Gil-Alana, L., Plastun, A., 2018. Persistence in the cryptocurrency market. *Research in International Business and Finance* 46, 141–148. doi:10.1016/j.ribaf.2018.01.002.
- Chapelle, A., Crama, Y., Hübner, G., Peters, J., 2005. Measuring and managing operational risk in financial sector: An integrated framework. *Social Science Research Network Electronic Journal* doi:10.2139/ssrn.675186.
- Choulakian, V., Stephens, M.A., 2001. Goodness-of-fit tests for the generalized pareto distribution. *Technometrics* 43, 478–484.
- Corbet, S., Lucey, B., Urquhart, A., Yarovaya, L., 2019. Cryptocurrencies as a financial asset: A systematic analysis. *International Review of Financial Analysis* 62, 182–199. doi:10.1016/j.irfa.2018.09.003.
- Corbet, S., Lucey, B.M., Peat, M., Vigne, S., 2018. Bitcoin futures - what use are they? *Economics Letters* 172, 23–27.
- Crama, Y., Hübner, G., Peters, J. (Eds.), 2007. Impact of the collection threshold on the determination of the capital charge for operational risk: *Advances in Risk Management*. Palgrave Macmillan, New York.
- Cramér, H., 1928. On the composition of elementary errors: Second paper: Statistical applications. *Scandinavian Actuarial Journal* 1, 141–180.
- Davison, A.C., 1984. *Modelling excess over high threshold, with an application: Statistical Extremes and Applications*. Reidel Publishing Company, Dordrecht, Netherlands. doi:10.1007/978-94-017-3069-3{\textunderscore}34.
- Davison, A.C., Smith, R.L., 1990. Models for exceedances over high thresholds (with comments). *Journal of the Royal Statistical Society, Series B (Methodological)* 52, 393–442.
- Dickey, D.A., Fuller, W.A., 1979. Distribution of the estimators for autoregressive time series with a unit root. *Journal of the American Statistical Association* 74, 427–431.

- Dyhrberg, A.H., 2016. Hedging capabilities of bitcoin. is it the virtual gold? *Finance Research Letters* 16, 139–144. URL: <https://www.sciencedirect.com/science/article/pii/S1544612315001208>, doi:10.1016/j.fr1.2015.10.025.
- ElBahrawy, A., Alessandretti, L., Kandler, A., Pastor-Satorras, R., Baronchelli, A., 2017. Evolutionary dynamics of the cryptocurrency market. *The Royal Society Open Science* 4.
- Embrechts, P., Klüppelberg, C., Mikosch, T., 1997. *Modelling Extremal Events: For Insurance and Finance*. *Applications of Mathematics, Stochastic Modelling and Applied Probability*, Springer Berlin Heidelberg. doi:10.1007/978-3-642-33483-2.
- Engle, R.F., 1982. Autoregressive conditional heteroscedasticity with estimates of the variance of united kingdom inflation. *Econometrica: Journal of the Econometric Society* 50, 987–1007. doi:10.2307/1912773.
- Engle, R.F., 2002. A simple class of multivariate generalized autoregressive conditional heteroskedasticity models. *Journal of Business & Economic Statistics* 20, 339–350.
- European Parliament, 2009. Directive 2009/138/ec of the european parliament and of the council of 25 november 2009 on the taking-up and pursuit of the business of insurance and reinsurance (solvency ii). *Official Journal of the European Union* 52, 1–155.
- European Parliament, 2013a. Directive 2013/36/eu of the european parliament and of the council of 26 june 2013 on access to the activity of credit institutions and the prudential supervision of credit institutions and investment firms, amending directive 2002/87/ec and repealing directives 2006/48/ec and 2006/49/ec and investment firms, amending directive 2002/87/ec and repealing directives 2006/48/ec and 2006/49/ec. *Official Journal of the European Union* 56, 338–436.
- European Parliament, 2013b. Regulation (eu) no 575/2013 of the european parliament and of the council of 26 june 2013 on prudential requirements for credit institutions and investment firms and amending regulation (eu) no 648/2012. *Official Journal of the European Union* 56, 1–337.
- Ferguson, T.S., 1967. *Mathematical statistics: A decision theoretic approach*. *Probability and mathematical statistics a series of monographs and textbooks*, 1, Academic Press, New York.
- Fry, J., Cheah, E.T., 2016. Negative bubbles and shocks in cryptocurrency markets. *International Review of Financial Analysis* 47, 343–352. doi:10.1016/j.irfa.2016.02.008.
- Gandal, N., Hamrick, J.T., Moore, T., Oberman, T., 2018. Price manipulation in the bitcoin ecosystem. *Journal of Monetary Economics* 95, 86–96.

- Gibbons, J.D., Chakraborti, S., 2011. Nonparametric statistical inference. volume 198 of *Statistics*. 5. ed. ed., Chapman & Hall/CRC Press, Boca Raton, Fla.
- Gkillas, K., Bekiros, S., Siriopoulos, C., 2018. Extreme correlation in cryptocurrency markets. SSRN Electronic Journal doi:10.2139/ssrn.3180934.
- Gkillas, K., Katsiampa, P., 2018. An application of extreme value theory to cryptocurrencies. *Economics Letters* 164, 109–111. doi:10.1016/j.econlet.2018.01.020.
- Glas, T.N., 2019. Investments in cryptocurrencies: Handle with care! *The Journal of Alternative Investments* 22, 96–113.
- Glivenko, V., 1933. Sulla determinazione empirica delle leggi di probabilità. *Giornale dell'Istituto Italiano degli Attuari* 1933, 92–99.
- Gnedenko, B.V., 1943. Sur la distribution limite du terme maximum d'une série aléatoire. *Annals of Mathematics* 44, 423–453.
- Hartigan, J.A., Hartigan, P.M., 1985. The dip test of unimodality. *The Annals of Statistics* 13, 70–84.
- Hayes, A.S., 2017. Cryptocurrency value formation: An empirical study leading to a cost of production model for valuing bitcoin. *Telematics & Informatics* 34, 1308–1321. doi:10.1016/j.tele.2016.05.005.
- Hoffmann, I., Börner, C., 2021. Body and tail: an automated tail-detecting procedure. *The Journal of Risk* 23, 43–69. doi:10.21314/JOR.2020.447.
- Hoffmann, I., Börner, C.J., 2018. Body and tail: Separating the distribution function by an efficient tail-detecting procedure in risk management. Working Paper .
- Hoffmann, I., Börner, C.J., 2020a. The risk function of the goodness-of-fit tests for tail models. *Statistical papers* , 1–17.
- Hoffmann, I., Börner, C.J., 2020b. Tail models and the statistical limit of accuracy in risk assessment. *The Journal of Risk Finance* 21, 201–216. doi:10.1108/JRF-11-2019-0217.
- Hosking, J.R.M., Wallis, J.R., 1987. Parameter and quantile estimation for the generalized pareto distribution. *Technometrics* 29, 339–349. doi:10.2307/1260343.
- Huisman, R., Koedijk, K.G., Kool, C.J.M., Palm, F., 2001. Tail-index estimates in small samples. *Journal of Business & Economic Statistics* 19, 208–216.
- Hull, J.C., 2018. Options, futures, and other derivatives. Ninth edition, global edition ed., Pearson Education, Harlow.

- Kakinaka, S., Umeno, K., 2020. Characterizing cryptocurrency market with lévy's stable distributions. *Journal of the Physical Society of Japan* 89, 024802. doi:10.7566/JPSJ.89.024802.
- Kaya Soyulu, P., Okur, M., Çatıkkaş, Ö., Altıntig, Z.A., 2020. Long memory in the volatility of selected cryptocurrencies: Bitcoin, ethereum and ripple. *Journal of Risk and Financial Management* 13, 107. doi:10.3390/jrfm13060107.
- Kendall, M.G., Stuart, A., 1977. *The advanced theory of statistics: In three volumes.* 4 ed., Charles Griffin & Co Ltd, London.
- Kolmogorov, A.N., 1933. Sulla determinazione empirica di una legge di distribuzione. *Giornale dell'Istituto Italiano degli Attuari* , 83–91.
- Longin, F., Solnik, B., 2001. Extreme correlation of international equity markets. *The Journal of Finance* 56, 649–676. doi:10.1111/0022-1082.00340.
- Majoros, S., Zempléni, A., 2018. Multivariate stable distributions and their applications for modelling cryptocurrency-returns. Working Paper 2018. URL: <http://arxiv.org/pdf/1810.09521v1>.
- von Mises, R.E., 1931. *Wahrscheinlichkeitsrechnung und ihre Anwendung in der Statistik und theoretischen Physik.* Franz Deuticke, Leipzig und Wien.
- Nakamoto, S., 2008. Bitcoin: A peer-to-peer electronic cash system. Consulted 1, 2012.
- Nolan, J.P., 2020. *Univariate Stable Distributions: Models for Heavy Tailed Data.* Springer Series in Operations Research and Financial Engineering. 1st ed. 2020 ed., Springer International Publishing and Imprint: Springer, Cham. doi:10.1007/978-3-030-52915-4.
- Osterrieder, J., Lorenz, J., Strika, M., 2017. Bitcoin and cryptocurrencies - not for the faint-hearted. *International Finance and Banking* 13, 145–193.
- Parr, W.C., Schucany, W.R., 1980. Minimum distance and robust estimation. *Journal of the American Statistical Association* 75, 616–624.
- Peng, Y., Albuquerque, P.H.M., Camboim de Sá, J.M., Padula, A.J.A., Montenegro, M.R., 2018. The best of two worlds: Forecasting high frequency volatility for cryptocurrencies and traditional currencies with support vector regression. *Expert Systems with Applications* 97, 177–192. doi:10.1016/j.eswa.2017.12.004.
- Pickands III, J., 1975. Statistical inference using extreme order statistics. *The Annals of Statistics* 3, 119–131. doi:10.1214/aos/1176343003.
- Polasik, M., Piotrowska, A.I., Wisniewski, T.P., Kotkowski, R., Lightfoot, G., 2015. Price fluctuations and the use of bitcoin: An empirical inquiry. *International Journal of Electronic Commerce* 20, 9–49.

- Schmitz, T., Hoffmann, I., 2020. Re-evaluating cryptocurrencies' contribution to portfolio diversification – a portfolio analysis with special focus on german investors. Working Paper URL: <http://arxiv.org/pdf/2006.06237v2>.
- Selgin, G., 2015. Synthetic commodity money. *Journal of Financial Stability* , 92–99.
- Shorack, G.R., Wellner, J.A., 2009. Empirical processes with applications to statistics. volume 59 of *Classics in applied mathematics*. Society for Industrial and Applied Mathematics, Philadelphia, Pa. URL: <http://www.loc.gov/catdir/enhancements/fy1001/2009025143-b.html>.
- Smirnov, N.V., 1936. Sur la distribution de w^2 -criterion (critérium de r. von mises). *Comptes Rendus de l'Académie des Sciences Paris* 202, 449–452.
- Smirnov, N.V., 1948. Table for estimating the goodness of fit of empirical distributions. *The Annals of Mathematical Statistics* 19, 279–281. doi:10.1214/aoms/1177730256.
- Smith, R.L., 1984. Threshold methods for sample extremes: Statistical extremes and applications 1984, 621–638.
- Smith, R.L., 1985. Maximum likelihood estimations in a class of nonregular cases. *Biometrika* 72, 67–90.
- Stephens, M.A., 1974. Edf statistics for goodness of fit and some comparisons. *Journal of the American Statistical Association* 69, 730–737. doi:10.2307/2286009.
- Trimborn, S., Li, M., Härdle, W.K., 2020. Investing with cryptocurrencies - a liquidity constrained investments approach: Working paper. *Journal of Financial Econometrics* 18, 280–306.
- Urquhart, A., 2018. What causes the attention of bitcoin? *Economics Letters* 166, 40–44.
- van Montfort, M.A.J., Witter, J.V., 1985. Testing exponentiality against generalized pareto distribution. *Journal of Hydrology* 78, 305–315.
- Wolfowitz, J., 1957. The minimum distance method. *The Annals of Applied Statistics* 28, 75–88.
- Wooldridge, J.M., 2020. *Introductory econometrics: A modern approach*. Seventh edition ed., CENGAGE, Boston, MA.